Power Flow Based Volt/var Optimization Under Uncertainty

Rabih A. Jabr, *Fellow*, *IEEE*

***Abstract*—Volt/var optimization (VVO) is a control function that is employed in distribution systems to keep the load voltages within the standard limits, and it includes secondary objectives such as loss minimization. The power flow based VVO is the way of choice in practical applications because it can handle a variety of objective functions and provides a solution even for large-scale network instances. This paper extends the power flow based VVO to account for uncertainty in both the load values and the power generation from photovoltaic sources. The proposed method employs circular arithmetic in complex variables to compute VVO settings that guard against load uncertainty and an optimized linear decision rule that modulates the reactive power of photovoltaic inverter in function of its active power. Finally, the proposed method is tested on distribution networks with up to 3146 nodes and is shown to produce optimal solutions that are robust against power variations.**

***Index Terms*—Circular arithmetic, optimization method, reactive power control, voltage control, Wirtinger calculus.**

I. Introduction

THE control of voltage and reactive power in modern distribution networks achieves the best performance when being carried out via a centralized system, as opposed to local automatic controllers. The local automatic controllers have their parameters computed using offline studies and therefore tend to be ineffective in many of the scenarios that are encountered in the practical operation. Centralized volt/var optimization (VVO) is a control function that is integrated into the system for supervisory control and data acquisition (SCADA) and the distribution management system (DMS). It makes use of a real-time network model derived from the result of the distribution system state estimator (DSSE). For the daily operation of the distribution network, the centralized VVO is commonly used in closed-loop mode; another option is the advisory mode that requires the review of the operator before implementation [1].

In practical applications, the centralized VVO can be rule-based or power flow based, but both start from the system state as given by the DSSE. The rule-based method employs a pre-determined set of control rules derived from offline studies, while the power flow based method computes the optimal solution of an objective function using a multi-step discrete programming search [1], [2]. The multi-step discrete programming search operates on integer variables that represent the switched capacitor settings and the tap positions of load tap changers (LTCs) on substation transformers and step voltage regulators. A power flow program is used to check the optimality of the control settings throughout different steps of the search. The multi-step discrete programming search can handle different objective functions, and its performance scales well with the problem size when being coupled with the compensation technique [3] for speeding up the power flow solution. The increased level of distributed energy sources connected into some distribution systems has impacts on the voltage profile and therefore requires the reactive power from these sources to be part of the VVO solutions [4] - [7]. This is also under the new IEEE 1547-2018 standard for smart inverters [8]. Although gradient-based methods [7], [9] are known to produce sufficiently good solutions in practical applications, programs that employ mixed-integer optimization [10], [11] such as branch-and-cut can provide better solutions to VVO. However, their applicability is limited to relatively small networks. The power flow model in practical VVO applications can typically include a few thousand nodes, even for solving a subsystem of the whole distribution network [1], therefore the performance of the VVO in large-scale distribution networks is an important issue.

The periodicity of centralized VVO generally is up to 15 min. During this interval, the values of loads and power generation from photovoltaic (PV) sources can deviate from the estimates given by the DSSE and consequently employed in the VVO; such variations may give rise to significant voltage violations. A work-around is to cast the power flow model as a conic program and formulate the VVO problem using robust [12], chance-constrained [13], or data-driven stochastic [14] optimization theory. The solution in this case makes use of mixed-integer optimization, which also limits the sizes of the networks that could be practically handled. Also, the applicability of the conic power flow model is confined to radial networks, while the subsystems controlled by VVO may be weakly meshed [1]. The conic programming formulations also appear in mathematically accurate statements of the chance-constrained VVO under Gaussian error [15], in distribution agnostic VVO [16], [17], and in interval optimal power flow [18].

Manuscript received: March 3, 2020; accepted: June 28, 2020. Date of Cross-Check: June 28, 2020. Date of online publication: September 9, 2020.

R. A. Jabr (corresponding author) is with Electrical and Computer Engineering, American University of Beirut, Beirut, Lebanon (e-mail: rabih.jabr@aub.edu.lb).

DOI: 10.35833/MPCE.2020.000129

This paper extends the practical power flow based VVO to guard against uncertainty in the load and power generation from PV sources. Rather than having the demand modeled as a fixed value, it is considered to vary within a disc in the complex plane. The disc has its center at the forecasting value, and its radius is chosen to reflect the uncertainty in the actual load. The disc load model allows the multi-step discrete programming search to compute the radius of voltage variation via circular arithmetic [19], and consequently choose VVO settings that are robust against load fluctuations. The computation of the voltage radius is made possible by a new approximate expression for the voltage magnitude in terms of the complex load power, that is derived using Wirtinger calculus [20], [21]. In related work, [22] presents new closed-form second- and third-order Taylor series expansions for the power flow and voltage phasor solution, and then discusses the application of these equations using circular arithmetic. The approximate solutions in [22] are different from the voltage magnitude solution that forms the basis of the voltage radius computation. Given that PV sources only produce active power, the uncertainty of this value is handled by computing a linear decision rule that dispatches the reactive power of inverters in function of the PV active power [23] - [25]. The slope of the linear decision rule for each of the inverters is chosen to minimize the deviation of voltages from the VVO set-points, which is derived from the new approximation for the voltage magnitude and is given in closed form.

The proposed VVO method is tested on radial and weakly meshed distribution networks with up to 3146 nodes. Monte Carlo analysis shows that the VVO solution computed under uncertainty is immune to power injection variations, contrary to the classical multi-step discrete programming search.

II. Centralized VVO

Centralized VVO can be used to optimize any mathematical function that aligns with the operation objectives of the distribution network. One possible function to be minimized involves the sum of the power loss and a penalty term for voltage magnitudes that violate their minimum/maximum limits [1]:

$$f = P_{Loss} + C_V \sum_{j=2}^{n} \max\left(0, |V_j| - |V_j|_{\max}\right) + C_V \sum_{j=2}^{n} \max\left(0, |V_j|_{\min} - |V_j|\right) \quad (1)$$

where P_{Loss} is the active power loss of the network; $|V_j|$ is the voltage magnitude at node j; n is the number of nodes; C_V is the penalty coefficient for voltage violation; and $|V_j|_{\min}$ and $|V_j|_{\max}$ are the minimum and maximum voltage magnitude limits, respectively. Reference [9] gives an explicit optimization problem statement of centralized VVO. The function in (1) is practically minimized by adjusting the tap positions of LTCs on substation transformers and step voltage regulators, the settings of switched capacitors, and the reactive power from distributed generation units such as PV inverters. The optimization is carried out using a multi-step discrete programming search, technically known as the discrete coordinate descent (DCD) algorithm [2], [9]. As its name indicates, the DCD algorithm updates the decision variables in discrete steps, and therefore, its application to VVO requires discretizing the range of reactive power generation from PV inverters. The flowchart of the DCD search for VVO is given in Fig. 1, where the following indexes are employed: ① best search direction (BSD); ② coordinate descent iteration (CDI) counter; ③ current/initial objective function (COF/IOF) value; ④ number of search direction (NSD); ⑤ search direction (SD).

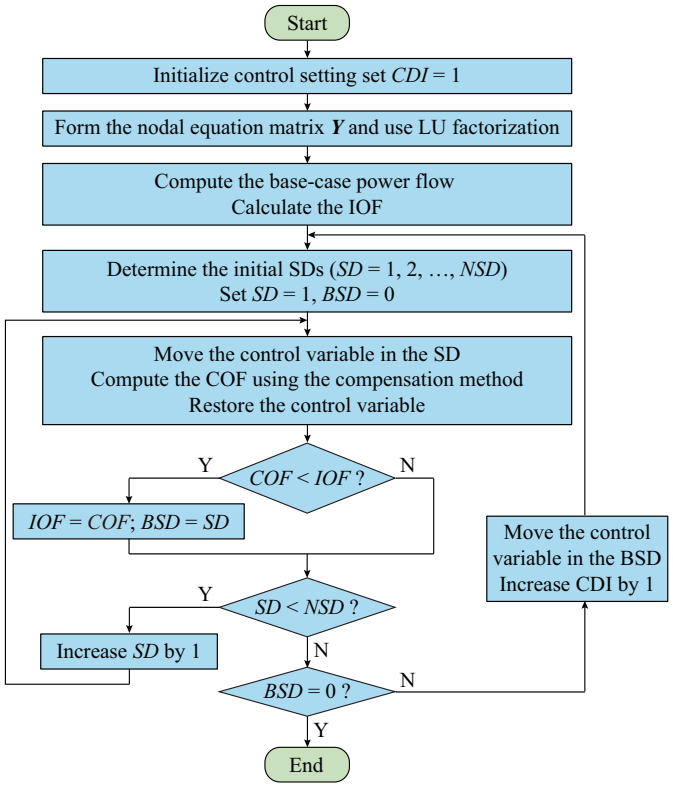

Fig. 1. Flowchart of DCD search for VVO.

The DCD algorithm starts by initializing the control settings of LTC transformer taps, switched capacitors, and reactive power from PV inverters. The initial values could be either the current operational ones or the nearest rounded ones computed from continuous optimization [9]. The nodal equation matrix $\boldsymbol{Y}$ is then formed, and LU factorization is used. The same LU factors are subsequently used to calculate the power flow following any changes in the control setting of the LTC taps and switched capacitors using the current injection power flow assisted by the compensation technique [3]. For the initial control settings, the DCD algorithm computes the IOF from the power flow results and then enumerates the possible SDs for each of the coordinates or decision variables. The search directions for a discrete variable are typically one step up in the control setting and one step down unless the variable has already been at one of its limits. The algorithm then computes the COF for each of the search directions and updates the values of the IOF and BSD whenever there is an improvement in the objective function value, i. e., when $COF < IOF$. The DCD search ends when it cannot find an im-

provement in the objective function value after it processes all the SDs at the current operation point.

VVO is a problem with a non-convex search space and discrete decision variables. Therefore, the DCD search may converge only to a local optimum, close to the initial operation point, but in line with the practical necessity of reduced controller switching. The DCD search forms the basis for considering uncertainty as described below.

III. Power Injection Uncertainty

The previous DCD search for VVO computes the control settings for a snapshot of the system that corresponds to the estimated (constant power) complex load and the active power generation from PV inverters. Therefore, the performance of the VVO is expected to deteriorate as the power injections deviate from their estimated values over the time interval between the control set-points in the field. In practice, this may translate into voltages operating outside their bounds. This section proposes a method that hedges the VVO against power injection uncertainty. The method builds on a linear approximate relationship between the nodal voltage magnitude and the complex power injections.

A. Voltage Magnitude Approximation

Consider the network shown in Fig. 2, where the first node is the slack node with the scheduled substation voltage V_1 and nodes 2 to n have their complex power injections $(S_2, S_3, \ldots, S_n)$ specified. The voltage magnitude at node j can be expressed in terms of the complex nodal voltage V_j and its conjugate $\bar{V}_j$:

$$\left|V_j\right| = \sqrt{V_j \bar{V}_j} \tag{2}$$

where the bar sign indicates the complex conjugation.

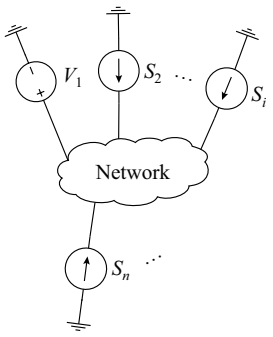

Fig. 2. Network with complex power injections and a slack node.

By using Wirtinger calculus [20], $\left|V_j\right|$ can be approximated by a first-order Taylor series expansion:

$$\left|V_j\right| = \sqrt{V_{j0}\bar{V}_{j0}} + \sum_{k=2}^{n} \frac{1}{2} \sqrt{\frac{\bar{V}_{j0}}{V_{j0}}} \left(\frac{\partial V_j}{\partial S_k} \Delta S_k + \frac{\partial V_j}{\partial \bar{S}_k} \Delta \bar{S}_k \right) + \sum_{k=2}^{n} \frac{1}{2} \sqrt{\frac{V_{j0}}{\bar{V}_{j0}}} \left(\frac{\partial \bar{V}_j}{\partial S_k} \Delta S_k + \frac{\partial \bar{V}_j}{\partial \bar{S}_k} \Delta \bar{S}_k \right) \tag{3}$$

where V_{j0} is the complex nodal voltage at the network operation point and the partial derivatives are evaluated at the same point. Exchanging terms between the summations in (3) results in:

$$\left|V_j\right| = \left|V_{j0}\right| + \overline{\sum_{k=2}^{n} \frac{1}{2} \left(\sqrt{\frac{\bar{V}_{j0}}{V_{j0}}} \frac{\partial V_j}{\partial \bar{S}_k} + \sqrt{\frac{V_{j0}}{\bar{V}_{j0}}} \frac{\partial \bar{V}_j}{\partial \bar{S}_k} \right) \Delta \bar{S}_k} + \sum_{k=2}^{n} \frac{1}{2} \left(\sqrt{\frac{\bar{V}_{j0}}{V_{j0}}} \frac{\partial V_j}{\partial \bar{S}_k} + \sqrt{\frac{V_{j0}}{\bar{V}_{j0}}} \frac{\partial \bar{V}_j}{\partial \bar{S}_k} \right) \Delta \bar{S}_k \tag{4}$$

Equation (4) can be written in terms of the real part $\mathrm{Re}\{\cdot\}$ of a complex quantity:

$$\left|V_j\right| = \left|V_{j0}\right| + \mathrm{Re}\left\{ \sum_{k=2}^{n} \left(\sqrt{\frac{\bar{V}_{j0}}{V_{j0}}} \frac{\partial V_j}{\partial \bar{S}_k} + \sqrt{\frac{V_{j0}}{\bar{V}_{j0}}} \frac{\partial \bar{V}_j}{\partial \bar{S}_k} \right) \Delta \bar{S}_k \right\} \tag{5}$$

To obtain the values of the partial derivatives in (5), i.e., $\partial V_j / \partial \bar{S}_k$ and $\partial \bar{V}_j / \partial \bar{S}_k$, at the current operation point, the nodal equations for the network are considered as specified in Fig. 2:

$$\boldsymbol{Y}\boldsymbol{V} = \boldsymbol{I} \tag{6}$$

$$\boldsymbol{Y} = \begin{bmatrix} 1 & 0 & \cdots & 0 & \cdots & 0 \\ Y_{21} & Y_{22} & \cdots & Y_{2k} & \cdots & Y_{2n} \\ \vdots & \vdots & & \vdots & & \vdots \\ Y_{k1} & Y_{k2} & \cdots & Y_{kk} & \cdots & Y_{kn} \\ \vdots & \vdots & & \vdots & & \vdots \\ Y_{n1} & Y_{n2} & \cdots & Y_{nk} & \cdots & Y_{nn} \end{bmatrix} \tag{7}$$

$$\begin{cases} \boldsymbol{V} = [V_1 \quad V_2 \quad \cdots \quad V_k \quad \cdots \quad V_n]^{\mathrm{T}} \\ \boldsymbol{I} = [V_s \quad \bar{S}_2/\bar{V}_2 \quad \cdots \quad \bar{S}_k/\bar{V}_k \quad \cdots \quad \bar{S}_n/\bar{V}_n]^{\mathrm{T}} = \begin{bmatrix} V_s \\ \bar{\boldsymbol{S}}_{pq} \oslash \bar{\boldsymbol{V}}_{pq} \end{bmatrix} \end{cases} \tag{8}$$

where V_s is the scheduled slack node voltage; $\boldsymbol{S}_{pq}$ and $\boldsymbol{V}_{pq}$ are column vectors containing the complex power injections and voltages at nodes 2 to n, respectively; and $\oslash$ denotes the Hadamard (element-by-element) division. Taking the partial derivative of (6) with respect to S_k $(k = 2, 3, \ldots, n)$, we can obtain:

$$\boldsymbol{Y} \partial \boldsymbol{V} / \partial S_k = \partial \boldsymbol{I} / \partial S_k \tag{9}$$

$$\partial \boldsymbol{I} / \partial S_k = \begin{bmatrix} 0 \\ -\left(\bar{\boldsymbol{S}}_{pq} \oslash \bar{\boldsymbol{V}}_{pq}^{\circledcirc 2} \right) \odot \partial \bar{\boldsymbol{V}}_{pq} / \partial S_k \end{bmatrix} \tag{10}$$

where $\odot$ and $\circledcirc$ denote the Hadamard product and power, respectively. Similarly, taking the partial derivative of the conjugate of (6) with respect to S_k $(k = 2, 3, \ldots, n)$, we can obtain:

$$\bar{\boldsymbol{Y}} \partial \bar{\boldsymbol{V}} / \partial S_k = \partial \bar{\boldsymbol{I}} / \partial S_k \tag{11}$$

$$\partial \bar{\boldsymbol{I}} / \partial S_k = \boldsymbol{v}_k + \begin{bmatrix} 0 \\ -\left(\boldsymbol{S}_{pq} \oslash \boldsymbol{V}_{pq}^{\circledcirc 2} \right) \odot \partial \boldsymbol{V}_{pq} / \partial S_k \end{bmatrix} \tag{12}$$

where $\boldsymbol{v}_k$ is an $n \times 1$ vector of zeros except for element k that has the value $1/V_k$. Combining (9)-(12), we can obtain the following system of equations:

$$\begin{bmatrix} \boldsymbol{Y} & \mathcal{D}\left\{ \begin{bmatrix} 0 \\ \bar{\boldsymbol{S}}_{pq} \oslash \bar{\boldsymbol{V}}_{pq}^{\circledcirc 2} \end{bmatrix} \right\} \\ \mathcal{D}\left\{ \begin{bmatrix} 0 \\ \boldsymbol{S}_{pq} \oslash \boldsymbol{V}_{pq}^{\circledcirc 2} \end{bmatrix} \right\} & \bar{\boldsymbol{Y}} \end{bmatrix} \begin{bmatrix} \partial \boldsymbol{V} / \partial S_k \\ \partial \bar{\boldsymbol{V}} / \partial S_k \end{bmatrix} = \begin{bmatrix} \boldsymbol{0}_{n \times 1} \\ \boldsymbol{v}_k \end{bmatrix} \tag{13}$$

where $\mathcal{D}\{\cdot\}$ is the diagonal matrix operator that converts a vector to a square diagonal matrix with the elements of the vector on the main diagonal. The solution to (13) is the partial derivatives in the column vectors $\partial \boldsymbol{V}/\partial S_k$ and $\partial \bar{\boldsymbol{V}}/\partial S_k$. Cosidering (14), the complex conjugate of this solution gives the coefficients needed in (5) [20].

$$\begin{cases} \partial \boldsymbol{V}/\partial \bar{S}_k = \overline{\partial \bar{\boldsymbol{V}}/\partial S_k} \\ \partial \bar{\boldsymbol{V}}/\partial \bar{S}_k = \overline{\partial \boldsymbol{V}/\partial S_k} \end{cases} \tag{14}$$

B. Load Uncertainty

To model the load uncertainty, it is assumed that its complex power injection can vary within an uncertainty disk in the complex plane. The center of this disk is at the forecasting load value S_k from the DSSE, and its radius ρ_{S_k} is chosen based on historical observations as a fraction of the apparent power. Therefore, the variation over the predicted value lies within a disk centered at the origin and with radius ρ_{S_k}. It can be defined by the following circular complex interval [19]:

$$\Delta S_k = \left\langle 0, \rho_{S_k} \right\rangle = \left\{ \Delta s_k \in \mathbb{C}, \left| \Delta s_k \right| \le \rho_{S_k} \right\} \tag{15}$$

where the two values in $\langle \cdot, \cdot \rangle$ are the center and radius, respectively. Equation (5) can be rewritten in compact form:

$$\left| V_j \right| = \left| V_{j0} \right| + \mathrm{Re}\left\{ \sum_{k=2}^{n} C_{jk} \Delta \bar{S}_k \right\} \tag{16}$$

$$C_{jk} = \sqrt{\frac{\bar{V}_{j0}}{V_{j0}}} \frac{\partial V_j}{\partial \bar{S}_k} + \sqrt{\frac{V_{j0}}{\bar{V}_{j0}}} \frac{\partial \bar{V}_j}{\partial \bar{S}_k} \tag{17}$$

Using circular arithmetic, $\sum_{k=2}^{n} C_{jk} \Delta \bar{S}_k$ is evaluated to a circular complex interval:

$$\sum_{k=2}^{n} C_{jk} \Delta \bar{S}_k = \left\langle 0, \rho_{|V_j|} \right\rangle \tag{18}$$

$$\rho_{|V_j|} = \sum_{k=2}^{n} \left| C_{jk} \right| \rho_{S_k} \tag{19}$$

Therefore, the approximation (16) for the voltage magnitude at node j decreases to a real interval:

$$\left| V_j \right| = \left[\left| V_{j0} \right| - \rho_{|V_j|}, \left| V_{j0} \right| + \rho_{|V_j|} \right] \tag{20}$$

Using the minimum and maximum limits of the real interval (20), the VVO objective function (1) can be modified to account for load uncertainty:

$$f = P_{Loss} + C_V \sum_{j=2}^{n} \max\left(0, \left| V_{j0} \right| + \rho_{|V_j|} - \left| V_j \right|_{\max}\right) + C_V \sum_{j=2}^{n} \max\left(0, \left| V_j \right|_{\min} - \left| V_{j0} \right| + \rho_{|V_j|}\right) \tag{21}$$

When using (21) in the DCD search in Fig. 1, $\rho_{|V_j|}$ is recomputed each time after the search direction is enumerated, i.e., after a change in a control variable setting is implemented.

C. PV Power Uncertainty

The DCD search in Fig. 1 produces the reactive power q_{k0} amongst other quantities, which should be dispatched from an inverter producing active power p_{k0}. The uncertainty in the PV active power production Δp_k is modeled by having it vary in a real interval ΔP_k, i.e.,

$$\Delta P_k = \left[\Delta P_k^{\min}, \Delta P_k^{\max} \right] = \left\{ \Delta p_k \in \mathbb{R}, \Delta P_k^{\min} \le \Delta p_k \le \Delta P_k^{\max} \right\} \tag{22}$$

where $\Delta P_k^{\min} < 0 < \Delta P_k^{\max}$. To mitigate the effect of the PV active power variability on voltage excursions, the reactive power of inverters can be adjusted following an affine decision rule [23]-[25]:

$$\Delta q_k = \alpha_k \Delta p_k \tag{23}$$

where α_k is the slope, which is a constant that can be optimally chosen and communicated to the inverter together with q_{k0}. Then, (16) can be used to estimate the voltage magnitude variation at node j corresponding to a change in the complex power injection from a PV inverter at node k:

$$\left| \Delta V_{jk} \right| = \left| V_{jk} \right| - \left| V_{j0} \right| = \mathrm{Re}\left\{ C_{jk} \left(\Delta p_k - \mathrm{i} \Delta q_k \right) \right\} = C_{jk}^r \Delta p_k + C_{jk}^i \Delta q_k = \left(C_{jk}^r + C_{jk}^i \alpha_k \right) \Delta p_k \tag{24}$$

where C_{jk}^r and C_{jk}^i are the real and imaginary parts of C_{jk} as computed in (17), respectively. The optimal value of α_k is calculated by minimizing the effect of Δp_k on the sum of voltage deviations (24) squared over all nodes, i.e.,

$$\min_{\alpha_k} \sum_{j=2}^{n} \left(C_{jk}^r + C_{jk}^i \alpha_k \right)^2 \tag{25}$$

The closed-form solution is obtained by taking the derivative of (25) with respect to α_k and setting it to be zero:

$$\alpha_k = -\frac{\sum_{j=2}^{n} C_{jk}^r C_{jk}^i}{\sum_{j=2}^{n} \left(C_{jk}^i \right)^2} \tag{26}$$

Using (26), the reactive power contribution from the inverter at node k becomes:

$$q_k = q_{k0} + \alpha_k \Delta p_k \tag{27}$$

If the apparent power capacity of inverters is $s_k^{\max}$, then the corresponding active power $p_k = p_{k0} + \Delta p_k$ and reactive power (27) have to satisfy [26]:

$$p_k^2 + q_k^2 \le \left(s_k^{\max} \right)^2 \tag{28}$$

$$-\sqrt{\left(s_k^{\max} \right)^2 - p_k^2} \le q_k \le \sqrt{\left(s_k^{\max} \right)^2 - p_k^2} \tag{29}$$

Thus, if q_k from (27) does not satisfy (29), then it is fixed at the violated limit.

IV. VVO Implementation

The three methods listed below are implemented for comparison.

1) Method 1 (M1): the DCD search in Fig. 1 is used to solve the VVO problem without considering the uncertainty in the values of the load, and the reactive power from each PV inverter is held constant at the optimized setting indepen-

dent of the changes in PV active power generation (to the maximum extent that (29) allows). M1 is essentially the same as Roytelman's DCD implementation discussed in [9].

2) Method 2 (M2): the DCD search in Fig. 1 is used to solve the VVO problem without considering the uncertainty in the values of the load, but the reactive power from each PV inverter is adjusted for variations in active power generation as described in Section III-C, i.e., according to the linear decision rule and the PV inverter capacity (26)-(29). M2 is essentially similar to the approach recently proposed in [25], which adopts a linear decision rule based on a linear approximation from the Newton-Raphson power flow Jacobean.

3) Method 3 (M3): the DCD search in Fig. 1 is used to solve the VVO problem while accounting for the uncertainty in the values of the load using circular arithmetic as described in Section III-B, and the reactive power from each PV inverter is adjusted for variations in active power generation as described in Section III-C.

V. Numerical Result

The VVO implementations (M1, M2, and M3) are tested on four networks, which include modified radial version (B_R) and modified meshed version (B_M) of a Brazilian distribution network in addition to two more extensive meshed networks with 1464 and 3146 nodes, which are denoted as 1k5 and 3k, respectively. Table I includes a summary of the test data, showing the number of nodes (n), the number of switched capacitors (N_{CAP}), the number of load tap changing transformers (N_{LTC}), the number of PV inverters (N_{PV}), the PV active power generation as a percentage of the total real load in the system snapshot (P_{PV}), and the ratio of the inverter apparent power capacity to the connected capacity of PV real power (R). The complete data sets of the test systems in Table I are available by downloading from [27]. In the simulation setup, it is assumed that the complex power load can vary in an uncertainty disc whose radius is at 5% of the estimated apparent power load value and that the PV active power generation can change by ±20% of the estimated value from the DSSE. Moreover, with the 20% variation, the PV system would generate active power at its connected capacity level. The uncertainty values reflect the differences that can occur in the power injections relative to their estimates, during the interval before the VVO setpoints are re-implemented in the field.

TABLE I
Test System Data

Network	n	N_{CAP}	N_{LTC}	N_{PV}	P_{PV}(%)	R
B_R	161	2	6	7	57.47	1.35
B_M	160	2	6	7	57.47	1.35
1k5	1464	8	8	5	68.51	1.10
3k	3146	13	15	10	84.10	1.10

Table II shows the reduction percentage in power loss from the VVO controller settings when the load and PV active power generation remain at their nominal DSSE values.

TABLE II
Reduction Percentage in Power Loss when Injections Remain at Nominal Values

Network	Reduction percentage (%)		
	M1	M2	M3
B_R	23.54	23.54	23.14
B_M	23.38	23.38	22.96
1k5	11.50	11.50	9.38
3k	20.32	20.32	18.16

In this ideal scenario, M1 and M2 realize the same reduction in loss value that is higher than that of M3, i.e., M3 appears at a disadvantage. The benefit of accounting for uncertainty in the VVO solutions, as in M2 and M3, is apparent whenever the injections deviate from their nominal values. A Monte Carlo simulation is carried out with 1000 trials of load and PV active power uniformly chosen from the abovementioned uncertainty sets. Half of the trials consider conforming load variations chosen from the peripheries of the uncertainty discs, while the other half do not. The results of the simulations are summarized in Tables III-V that quantify the effects of M2 and M3 on the robustness of the VVO settings.

TABLE III
Average Total Voltage Violation at All Nodes Observed from 1000 Trials

Network	Average total voltage violation (p.u.)		
	M1	M2	M3
B_R	1.37×10^{-2}	8.22×10^{-4}	1.55×10^{-5}
B_M	1.39×10^{-2}	7.67×10^{-4}	1.36×10^{-5}
1k5	6.54×10^{-1}	2.32×10^{-1}	1.77×10^{-7}
3k	1.44×10^{0}	9.01×10^{-1}	5.63×10^{-5}

TABLE IV
Average Percentage of Nodes with Voltage Violations Observed from 1000 Trials

Network	Average percentage (%)		
	M1	M2	M3
B_R	3.30	0.77	0.05
B_M	3.22	0.65	0.05
1k5	6.84	4.06	0
3k	7.48	6.16	0

TABLE V
Number of Nodes with Voltage Violations Observed from 1000 Trials

Network	Number of nodes		
	M1	M2	M3
B_R	17	7	4
B_M	16	5	2
1k5	522	289	1
3k	1196	868	6

Tables III and IV show the average total voltage violation at all nodes and the average percentage of nodes with voltage violations observed from the 1000 trials. As expected, M3 has the best results measured by the extent of mitigating voltage violations, followed by M2. Table V lists the maximum observed number of nodes with voltage violations, and again shows the vast superiority of M3. The effect of M3 on power loss is shown in Table VI, which reports the percentage increase in power loss relative to centralized optimization, i.e., when the VVO problem is centrally re-solved for the reactive power of PV inverter corresponding to each of the sampled trials. The effect of using the linear decision rule (Section III-C) comes at the maximum cost of 2.62% increase in loss for the 3k.

TABLE VI
PERCENTAGE INCREASE IN POWER LOSS USING M3 RELATIVE TO CENTRALIZED OPTIMIZATION OBSERVED FROM 1000 TRIALS

Network	Percentage increase in power loss (%)
B_R	0.55
B_M	0.59
1k5	2.12
3k	2.62

In terms of computation time, the largest network is solved in less than 1 min using M1 and M2, and less than 13 min using M3. The computation time is recorded using a MATLAB implementation running on a MacBook Pro that has 2.9 GHz Intel Core i5 processor with a memory of 8 GB 2133 MHz.

A central aspect of M3 is the computation of the voltage radius. A Monte Carlo simulation with 10000 trials is used to validate the closed-form solution for the voltage magnitude radius $\rho_{|V_j|}$, as given by (19). In each experiment, the nodal complex power injections are sampled from the boundaries of the uncertainty discs, and the current injection power flow is used to find the voltage solution of the trial and its distance from the nominal solution. The radius $\rho^{MCS}_{|V_j|}$ at each node is computed as the maximum distance observed over the 10000 trials. To quantify the accuracy of the radius computation (19), the relative error at each node is defined by (30) or (31).

$$\rho^{r.e}_{|V_j|} = \frac{\left|\left(|V_j| + \rho^{MCS}_{|V_j|}\right) - \left(|V_j| + \rho_{|V_j|}\right)\right|}{|V_j| + \rho^{MCS}_{|V_j|}} \times 100 \tag{30}$$

$$\rho^{r.e}_{|V_j|} = \frac{\left|\rho^{MCS}_{|V_j|} - \rho_{|V_j|}\right|}{|V_j| + \rho^{MCS}_{|V_j|}} \times 100 \tag{31}$$

Table VII shows the maximum and average values of the relative error over all nodes when computed for the network state before and after the VVO solution. The results verify the accuracy of the proposed solution (19).

TABLE VII
RELATIVE ERROR OF VOLTAGE MAGNITUDE RADIUS

Network	Relative error (%)			
	Before VVO		After VVO	
	Average	Maximum	Average	Maximum
B_R	0.0059	0.0295	0.0044	0.0193
B_M	0.0057	0.0295	0.0043	0.0192
1k5	0.1008	0.4024	0.0643	0.3470
3k	0.1287	0.5283	0.0739	0.4618

VI. CONCLUSION

Centralized VVO is practically solved using a multi-step discrete programming search that gives a solution corresponding to the estimated power injections, involving loads and power from PV sources. This paper proposes a methodology for extending the classical VVO solution to account for the uncertainty in the power injections during the time interval when the VVO control settings are applicable. The method is two-pronged and aims to alleviate voltage magnitude violations. It involves the use of circular arithmetic to guard against load variations and a linear decision rule that tailors the reactive power of PV inverters in function of its active power. Both components of the solution that combats uncertainty are fundamentally based on a linear approximated relationship between the nodal voltage magnitude and complex power injections. The relation is a complex variable first-order Taylor series expansion of the voltage magnitude, derived by Wirtinger calculus. The proposed method is tested on distribution networks with up to 3146 nodes and compared with the techniques that either neglect uncertainty altogether [9] or only account for PV active power uncertainty [25]. The numerical comparison shows that the proposed method is significantly better in terms of the quality of delivered power, and yet keeps the energy losses within an acceptable margin from an ideal centralized inverter dispatching solution.

REFERENCES

[1] I. Roytelman and J. M. Palomo. (2016, May). Volt/var control in distribution systems. [Online]. Available: http://digital-library. theiet.org/content/books/10.1049/pbpo075e_ch8

[2] I. Roytelman, B. K. Wee, and R. L. Lugtu, "Volt/var control algorithm for modern distribution management system," *IEEE Transactions on Power Systems*, vol. 10, no. 3, pp. 1454-1460, Aug. 1995.

[3] W. F. Tinney, "Compensation methods for network solutions by optimally ordered triangular factorization," *IEEE Transactions on Power Apparatus and Systems*, vol. PAS-91, no. 1, pp. 123-127, Jan. 1972.

[4] M. Juamperez, G. Yang, and S. B. KJÆR, "Voltage regulation in LV grids by coordinated volt-var control strategies," *Journal of Modern Power Systems and Clean Energy*, vol. 2, no. 4, pp. 319-328, Dec. 2014.

[5] G. Yang, F. Marra, M. Juamperez *et al*., "Voltage rise mitigation for solar PV integration at LV grids," *Journal of Modern Power Systems and Clean Energy*, vol. 3, no. 3, pp. 411-421, Sept. 2015.

[6] E. Ghiani and F. Pilo, "Smart inverter operation in distribution networks with high penetration of photovoltaic systems," *Journal of Modern Power Systems and Clean Energy*, vol. 3, no. 4, pp. 504-511, Dec. 2015.

[7] Y. Shi and M. Baran, "A gradient based decentralized volt/var optimization scheme for distribution systems with high DER penetration," in *Proceedings of 2019 IEEE PES GTD Grand International Conference*

and Exposition Asia (GTD Asia), Bangkok, Thailand, Mar. 2019, pp. 649-654.

[8] IEEE PES Industry Technical Support Task Force. (2018, May). Impact of IEEE 1547 standard on smart inverters. [Online]. Available: https://resourcecenter. ieee-pes. org/publications/technical-reports/PES_TR0067_5-18.html

[9] R. A. Jabr and I. Džafić, "Sensitivity-based discrete coordinate-descent for volt/var control in distribution networks," *IEEE Transactions on Power Systems*, vol. 31, no. 6, pp. 4670-4678, Nov. 2016.

[10] A. Borghetti, "Using mixed integer programming for the volt/var optimization in distribution feeders," *Electric Power System Research*, vol. 98, pp. 39-50, May 2013.

[11] A. Borghetti, F. Napolitano, and C. A. Nucci, "Volt/var optimization of unbalanced distribution feeders via mixed integer linear programming," *International Journal of Electrical Power & Energy Systems*, vol. 72, pp. 40-47, Nov. 2015.

[12] T. Ding, S. Liu, W. Yuan *et al*., "A two-stage robust reactive power optimization considering uncertain wind power integration in active distribution networks," *IEEE Transactions on Sustainable Energy*, vol. 7, no. 1, pp. 301-311, Jan. 2016.

[13] F. U. Nazir, B. C. Pal, and R. A. Jabr, "A two-stage chance constrained volt/var control scheme for active distribution networks with nodal power uncertainties," *IEEE Transactions on Power Systems*, vol. 34, no. 1, pp. 314-325, Jan. 2019.

[14] T. Ding, Q. Yang, Y. Yang *et al*., "A data-driven stochastic reactive power optimization considering uncertainties in active distribution networks and decomposition method," *IEEE Transactions on Smart Grid*, vol. 9, no. 5, pp. 4994-5004, Sept. 2018.

[15] K. S. Ayyagari, N. Gatsis, and A. F. Taha, "Chance constrained optimization of distributed energy resources via affine policies," in *Proceedings of 2017 IEEE Global Conference on Signal and Information Processing*, Montreal, Canada, Nov. 2017, pp. 1050-1054.

[16] K. Baker, E. Dall'Anese, and T. Summers, "Distribution-agnostic stochastic optimal power flow for distribution grids," in *Proceedings of 2016 North American Power Symposium (NAPS)*, Denver, USA, Sept. 2016, pp. 1-6.

[17] L. Dong, J. Li, T. Pu *et al*., "Distributionally robust optimization model of active distribution network considering uncertainties of source and load," *Journal of Modern Power Systems and Clean Energy*, vol. 7, no. 6, pp. 1585-1595, Nov. 2019.

[18] P. Chen, X. Xiao, and X. Wang, "Interval optimal power flow applied to distribution networks under uncertainty of loads and renewable resources," *Journal of Modern Power Systems and Clean Energy*, vol. 7, no. 1, pp. 139-150, Jan. 2019.

[19] I. Gargantini and P. Henrici, "Circular arithmetic and the determination of polynomial zeros," *Numerische Mathematik*, vol. 18, no. 4, pp. 305-320, Aug. 1971.

[20] K. Kreutz-Delgado. (2009, Jun.). The complex gradient operator and the CRcalculus. [Online]. Available: http://arxiv.org/abs/0906.4835

[21] I. Džafić, R. A. Jabr, and T. Hrnjić, "Hybrid state estimation in complex variables," *IEEE Transactions on Power Systems*, vol. 33, no. 5, pp. 5288-5296, Sept. 2018.

[22] R. A. Jabr, "High-order approximate power flow solutions and circular arithmetic applications," *IEEE Transactions on Power Systems*, vol. 34, no. 6, pp. 5053-5062, Nov. 2019.

[23] W. Lin, R. J. Thomas, and E. Bitar, "Real-time voltage regulation in distribution systems via decentralized PV inverter control," in *Proceedings of the 51st Hawaii International Conference on System Sciences*, Hawaii, USA, Jan. 2018, pp. 2680-2689.

[24] W. Lin and E. Bitar, "Decentralized stochastic control of distributed energy resources," *IEEE Transactions on Power Systems*, vol. 33, no. 1, pp. 888-900, Jan. 2018.

[25] R. A. Jabr, "Robust volt/var control with photovoltaics," *IEEE Transactions on Power Systems*, vol. 34, no. 3, pp. 2401-2408, May 2019.

[26] K. Turitsyn, P. Sulc, S. Backhaus *et al*., "Options for control of reactive power by distributed photovoltaic generators," *Proceedings of the IEEE*, vol. 99, no. 6, pp. 1063-1073, Jun. 2011.

[27] R. A. Jabr. (2020, Mar.). "VVO distribution network data sets," [Online]. Available: https://www. dropbox. com/s/pyi0tfatm8e353m/mpce_VVO.zip?dl=0

Rabih A. Jabr received the B.E. degree in electrical engineering (with high distinction) from the American University of Beirut, Beirut, Lebanon, in 1997, and the Ph.D. degree in electrical engineering from Imperial College London, London, U.K., in 2000. Currently, he is a Professor in the Department of Electrical and Computer Engineering, American University of Beirut. His research interests include mathematical optimization techniques and power system analysis and computing.